RSC Advances

PAPER

View Article Online
View Journal | View Issue

Cite this: *RSC Adv.*, 2021, **11**, 24429

A low-cost and high-loading viologen-based organic electrode for rechargeable lithium batteries†

Mao Chen,‡[a] Lei Liu,‡[b] Peiyao Zhang[a] and Hongning Chen *[a]

Organic active materials are regarded as a very promising choice for lithium batteries because of several outstanding advantages such as low-cost, flexible tunability and pollution-free sources. Viologen compounds are attractive two-electron storage materials with low redox potentials, which are mainly used as anolytes in redox flow batteries (RFBs) considering their high solubility in electrolytes. However, due to their relatively large molecular weight and low density, it is difficult to prepare high-loading and stable-cycling electrodes for lithium battery application. In this research, by adopting 4,4′-bipyridine as the raw material and combining salification with a high-energy ball milling method, a low-solubility and high-stability viologen carbon-coated composite, ethyl viologen dihexafluorophosphate-Ketjen black (EV-KB), is synthesized. Then, by optimizing the electrode preparation process, a high-loading viologen-based electrode is successfully prepared. Salification effectively reduces the solubility of viologen compounds in the electrolyte so that the EV-KB composite can be used in lithium batteries. At the same time, it is pointed out that current collectors and slurry solvents play an important role in achieving the high-loading electrode. By deliberately selecting carbon paper as the current collector and ethanol as the solvent, the EV-KB composite organic electrode with a loading up to 1.5–9 mg cm^{-2} can achieve a specific capacity of 106–79 mA h g^{-1} for 400 stable cycles with a coulombic efficiency of 96% as well as a good rate capability. The synthesis method and electrode preparation optimization process introduced in this paper provide a reference for other types of organic active materials to be used in high-loading lithium batteries.

Received 20th April 2021
Accepted 7th July 2021

DOI: 10.1039/d1ra03068j

rsc.li/rsc-advances

Introduction

With the increasing problem of environmental pollution, the demand for clean energy storage is becoming more and more urgent.[1–3] It is known that lithium-ion batteries are the most commercialized electrochemical energy storage device at present; therefore, the environmental protection ability of their electrode active materials has attracted most attention.[4–6] In traditional lithium-ion batteries, the active materials contain transition metal elements such as cobalt, titanium, and manganese, so that they are not only expensive but also harmful to the environment due to their toxicity.[7–10] Hence, developing a new type of low-cost and environment-friendly active materials has become significant for the better utilization of lithium-ion batteries in the future.

Currently, organic active materials are regarded as a very attractive choice for electrodes because of their low-cost, diversity of molecular moieties, wide range of reaction potential and pollution-free sources.[11–16] For example, quinone compounds, through appropriate molecular modification, can be synthesized to various derivatives and achieve a stable cycling performance in the potential range of 1.7 V to 3.2 V *vs.* Li/Li^+.[17–19] Many sources of quinone compounds can be found in nature. For example, there are many quinone derivatives involved in the electron transport chain of chloroplasts.[20,21] In addition, organic active materials such as pteridine,[22] nitroxyl radicals[23,24] and their derivatives[25] have also been used in batteries, showing excellent application prospects. Among these organic active materials, viologen-based active materials are attractive two-electron storage active materials with low redox potentials even if the molecular form of viologen is highly toxic.[24,26,27] However, they are now mainly used in RFBs because

[a]*Chemical Hybrid Energy Novel Laboratory, College of Chemistry and Environmental Engineering, Shenzhen University, Shenzhen, Guangdong, 518055, PR China. E-mail: hnchen@szu.edu.cn*

[b]*College of Chemistry and Materials Science, Anhui Normal University, Wuhu 241000, China*

† Electronic supplementary information (ESI) available: ^1H NMR of EV in D_2O, TGA of EV-KB composite, XPS spectra of EV-KB composite, EV-KB composite electrode preparation comparison and cell configuration, EV-KB composite electrode coating comparison, cycling performance of EV-KB composite electrode for 1st electron, cycling performance of EV-KB composite electrode for 2nd electron, cycling performance of EV-KB composite electrode with mass loading of 9 mg cm^{-2}, cycling performance of EV-KB composite electrode with mass loading of 1.5 mg cm^{-2}. See DOI: 10.1039/d1ra03068j

‡ These authors contributed equally to this work.

of their high solubility in electrolytes.[28] Viologen-based active materials can be applied in lithium batteries only if their solubility can be inhibited and their stability can be improved in the electrode.[29] Viologen-based active materials belong to p-type organics, which the reaction is between the neutral state and the positively charged state.[14] This structure leads to a dual-ion configuration relying on both cations and anions. Moreover, the molecular anions are generally used as charge carriers for compensation.[30,31] In recent years, salification has been taken as an effective method to suppress the dissolution of organic active materials, and it is able to improve the electrode cycle performance of the materials through the principle of reversing polarity.[32–34] Chen *et al.* used this method to successfully demonstrate two viologen salt compounds which achieved 200 stable cycles.[35] This study provides a good strategy for the application of viologen-based active materials in lithium batteries.

Developing high-loading electrodes is crucial for the practical battery application. In classic LIBs, the high-loading electrodes can be achieved by binder enhancement,[36] current collector optimization,[37] active material modification[38] and advanced electrode manufacturing.[39] However, the current research of organic electrode is mostly concentrated on developing novel active materials but often overlooks the importance of high-loading. Recent years, novel electrode architectures and electrode fabrication methods have been successfully applied to organic active materials.[40,41] For example, the carboxylate compound was designed to achieve high mass loading of 12.0 mg cm^{-2} with only 0.5 wt% carbon additive.[42] Nevertheless, large polarization and poor rate performance issues arise as the mass loading increases. The problems associated with high-loading of organic active materials still need to be addressed in the future. Due to the low density, high molecular weight and poor conductivity of organic active materials, it is difficult to achieve high-loading electrodes. Therefore, compared with the traditional lithium-ion battery electrode, the single cell capacity of organic active material electrode is much smaller, which is not conducive to its further application in more fields. Especially for today's vigorous development of electric vehicles, a higher requirement for the single cell capacity is put forward.[43–46] Among the reported work so far, the loading of the organic active material electrode is about 1–5 mg cm^{-2}, and there is still a lot of room for improvement. For the optimization of organic electrodes, many researchers embark on the preparation of composites,[47,48] the selection of binders[49,50] or solvents,[51] which makes the stability and loading of the electrode improved to a certain extent. For example, in the research of Cui and Bao *et al.*, the cycle performance of the organic active material disodium rhodizonate ($Na_2C_6O_6$) was successfully improved by optimizing the size of the active material and selecting the appropriate electrolyte.[52]

In this work, 4,4′-bipyridine is used as the raw material to synthesize viologen compounds by salification, and through ion exchange, the almost insoluble ethyl viologen dihexafluorophosphate ($EV(PF_6)_2$) is obtained, which can be effectively adopted as the electrode active material for lithium batteries. Then, EV-KB composite is prepared by a simple high-energy ball milling of $EV(PF_6)_2$ with conductive carbon Ketjen black (KB) to increase the conductivity and stability of the active material. After optimizing the electrode preparation process, a high-loading viologen-based organic electrode is achieved and applied to lithium batteries. Because the salification method can effectively reduce the solubility of EV in the electrolyte, the active material is no longer dissolved in the electrolyte, thereby improving its stability; at the same time, the EV-KB composite effectively increases the connection between the active materials, so that it can still achieve better cycle stability under high-loading conditions. In our demonstration, the EV-KB composite electrode is able to reach a specific capacity of 106–79 mA h g^{-1} with a high-loading of 1.5–9 mg cm^{-2}. It can also stably cycle 400 times under certain conditions with the coulombic efficiency of 96%. The synthesis method and electrode preparation optimization process adopted in this paper provide a reference for other types of organic active materials to be used in high-loading lithium batteries.

Experimental

Synthesis of ethyl viologen dihexafluorophosphate ($EV(PF_6)_2$)

4,4′-Bipyridine (1.000 g, 6.4 mmol) and bromoethane (1.746 g, 16.0 mmol) were mixed in acetonitrile (ACN, 15 mL) and stirred at 80 °C overnight. After cooling down at room temperature, the suspended solid was collected by filtration and rinsed with acetone for 3 times. Finally, faint yellow solid (**1**) was obtained after vacuum drying at 50 °C overnight (yield: 2.035 g, 85%).

1 (1.000 g, 2.7 mmol) and KPF_6 (2.945 g, 16.0 mmol) were mixed and stirred in DI water at room temperature overnight. Then the suspended solid was collected by vacuum filtration and rinsed with DI water. Finally, white solid ($EV(PF_6)_2$) was obtained after vacuum drying at 65 °C overnight (yield: 1.225 g, 90%).

Synthesis of EV-KB composite

EV-KB composite was prepared by a simple and scalable high-energy mechanical ball milling method. The synthesized $EV(PF_6)_2$ (EV) and Ketjen Black (KB) were mixed in the mass ratio of 2 : 1 in a zirconia vessel. Fritsch Pulverisette-6 was applied at a speed of 350 rpm with the milling duration of 30 min. The collected EV-KB composite was dried in oven at 55 °C overnight.

Preparation of EV-KB composite electrode

EV-KB composite electrodes were prepared by mixing EV-KB composite with PTFE binder in NMP/ethanol solvent (EV:KB:PTFE = 5.4 : 3.6 : 1). The mixtures were sonicated in an glass container to get homogeneous slurry and coated on a clean carbon paper/aluminum foil. After drying in a oven at 55 °C for 12 h, the samples were measured with a mass loading of 1.5–9 mg cm^{-2} for typical electrodes in Φ14 mm discs as shown in Fig. S4a.†

Assembly of Li-EV based coin cell

Fig. S4b† shows the structure of the Li-EV based coin cell (CR2032). The electrolyte used in the cell assembling was 1 M $LiClO_4$ in propylene carbonate (PC). One piece of lithium foil (Φ16 mm) was attached to a anode plate cell body, which acted as a current collector for the anode side. 50 μL of electrolyte was added on the surface of lithium foil. One glass fiber separator (Φ19 mm) was placed on the surface of the lithium foil followed by adding 50 μL of electrolyte. One piece of EV-KB composite electrode (Φ14 mm) was placed on the separator. Finally, a stainless steel spring and a cathode plate were placed on the cell. The cell assembling process was conducted in an Ar-filled glove box (Etelux, H_2O < 1.0 ppm, O_2 < 1.0 ppm).

Electrochemical characterizations

All the electrochemical characterizations were performed using the Bio-Logic VSP electrochemical workstation. Cyclic voltammogram (CV) tests of active materials (2 mM $EV(PF_6)_2$ in 1 M $LiClO_4$ PC or 1 M $LiPF_6$ EC/DEC electrolyte) were conducted between −2.0 and 0 V *vs.* Ag/Ag^+ using a three electrodes configuration with glassy carbon electrode as working electrode, nonaqueous Ag/Ag^+ electrode as reference electrode and Pt wire as counter electrode. Galvanostatic discharge–charge tests were performed between 1.5 and 3.0 V *vs.* Li/Li^+ for full cell. Voltage control galvanostatic discharge–charge tests were performed between 2.1 and 3.0 V *vs.* Li/Li^+ for 1st electron and 1.5 and 2.4 V *vs.* Li/Li^+ for 2nd electron. Current density was calculated based on the current collector geometric surface area. The specific capacity was calculated from the mass of active materials ($EV(PF_6)_2$).

Material characterizations

Scanning electron microscopy (SEM) and energy dispersive X-ray (EDX) characterization were performed on JEOL JSM-7800F. The X-ray photoelectron spectroscopy (XPS) test was conducted on K-Alpha+. Thermogravimetric analysis (TGA) was performed STA409PC (NETZSCH-Gerätebau GmbH). ^1H NMR was recorded on VarianVNMRS 400 in solutions of D_2O.

Results and discussion

In this paper, using 4,4′-bipyridine as the raw material, the viologen-based organic active material $EV(PF_6)_2$ is obtained through a two-step synthetic route (Fig. 1a). In this process, we note that Br^{-1} anions is replaced by PF_6^{-1} through ion exchange, which makes the synthesized viologen active material almost insoluble in the electrolyte. Thus, this material can be effectively used in the electrode of the lithium battery. We observed that the solubility of as-prepared $EV(PF_6)_2$ is around 5–10 mM in the 1 M $LiClO_4$ PC electrolyte with obvious precipitate as shown in Fig. S11.† The ^1H NMR results in Fig. S1† confirm the chemical structure and purity of the synthesized EV compound, proving the successful synthesis. We conducted the EDX and XPS tests of the as-prepared $EV(PF_6)_2$ to examine the structure after ion exchange process as shown in Fig. S13 and S14.† The results indicate that all the Br^- ions are replaced by

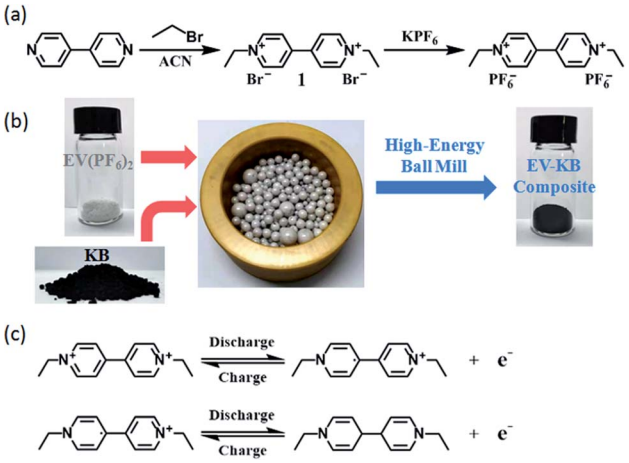

Fig. 1 (a) Schematic synthesis process of ethyl viologen dihexafluorophosphate ($EV(PF_6)_2$). (b) Schematic synthesis process of EV-KB composite. (c) Redox reaction mechanism of $EV(PF_6)_2$.

PF_6^- in our synthesis method. Viologen compounds are attractive organic active materials with two transfer electrons. As shown in Fig. 1c, during the discharge–charge process, the two N atoms on the benzene ring can each gain or lose an electron, thus realizing a reversible double electronic redox reaction, and providing two corresponding discharge–charge plateaus. Based on $EV(PF_6)_2$, a high-energy ball milling is then used to mix it with conductive carbon KB to prepare EV-KB composite, thereby increasing the conductivity and stability of $EV(PF_6)_2$ (Fig. 1b). The results of thermogravimetric analysis in Fig. S2† show that the yield of this method is very efficient, and the active material in the obtained EV-KB composite accounts for about 61% with almost no loss.

Compared with $EV(PF_6)_2$, the EV-KB composite synthesized by high-energy ball milling has more uniform particles and an obvious carbon-coated morphology, which makes it more conductive and more uniformly distributed when preparing electrodes. As shown in the SEM results of Fig. 2, after high-energy ball milling, the morphology of $EV(PF_6)_2$ aggregation is broken into smaller and more uniform particles. It can be seen from the EDX results of Fig. 2c that the C atoms and other

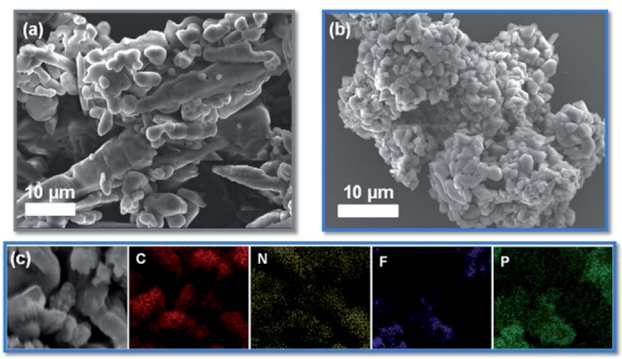

Fig. 2 SEM images of (a) $EV(PF_6)_2$ and (b) EV-KB composite. (c) EDX images of EV-KB composite.

atoms (N, F, P) in EV are uniformly distributed and overlapped throughout EV-KB composite, which proves the uniformity of EV-KB composite in coating carbon. This simple and efficient composite synthesis method can effectively improve the electrochemical performance of $EV(PF_6)_2$. Fig. 3a shows the cyclic voltammetry (CV) results of 2 mM $EV(PF_6)_2$ in 1 M $LiClO_4$ in PC at various scanning rates. It can be observed that the redox potentials of $EV(PF_6)_2$ are −0.82 V (EV/EV^+) and −1.22 V (EV^+/EV^{2+}) *vs.* Ag/Ag^+, respectively corresponding to the two-step reaction in Fig. 1c. In addition, the oxidation peaks and reduction peaks are very symmetrical, showing good reversibility. These two reactions come from the gain and loss of electrons of the two N atoms on the benzene ring. However, $EV(PF_6)_2$ exhibits poor reversibility in the commonly used 1 M $LiPF_6$ EC/DEC electrolyte as shown in Fig. S12.† The CV results shows asymmetrical configuration for the oxidation and reduction peaks, which implies that the 1 M $LiPF_6$ EC/DEC electrolyte is not suitable to be used in the EV based system. The structure of $EV(PF_6)_2$ is then confirmed through X-ray photoelectron spectroscopy (XPS). As shown in Fig. 3b and c, the characteristic peaks of C–C, C–H (284.6 eV) and C–N (285.0 eV) appear in the C 1s spectrum, and the characteristic peaks of N^+ (401.6 eV) and C–N (399.8 eV) appear in the N 1s spectrum, all of which are in line with the structural characteristics of $EV(PF_6)_2$. Meanwhile, similar results in the XPS of the EV-KB composite (Fig. S3†) are obtained, which suggests that after high-energy ball milling, the structure of the EV are not changed and its electrochemical properties are not affected. Moreover, there is a CF_3 (292.2 eV) peak in both $EV(PF_6)_2$ and EV-KB composite. This is mainly due to the small amount of impurities introduced in the ion exchange with KPF_6 during the synthesis.

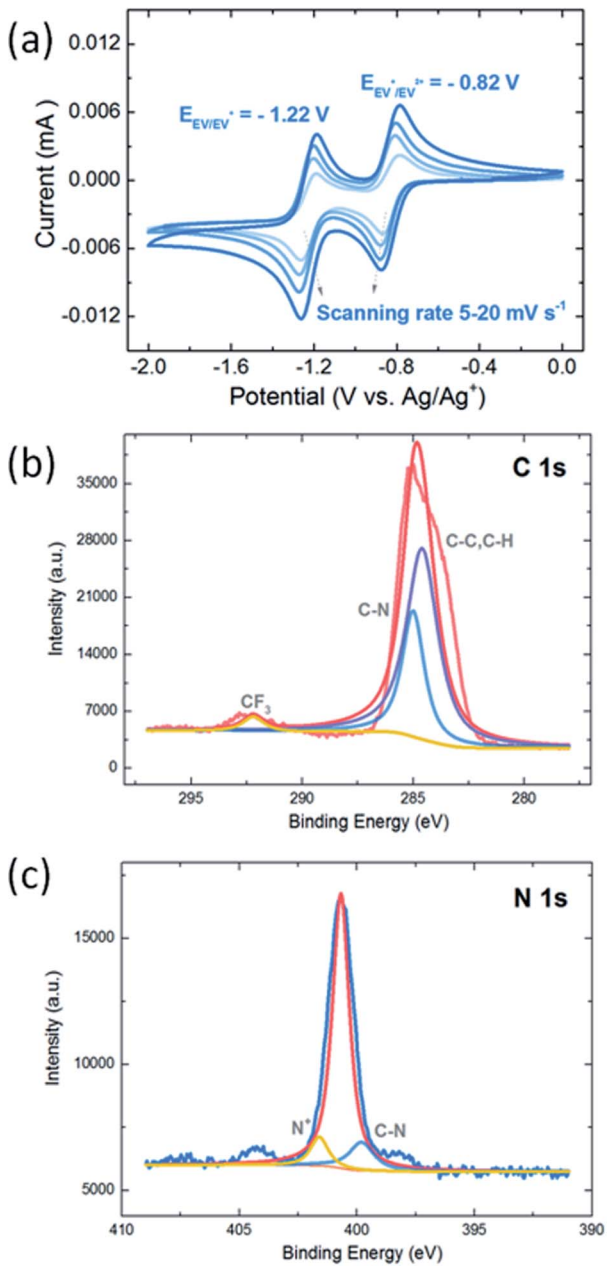

Fig. 3 (a) Cyclic voltammetry results of 2 mM $EV(PF_6)_2$ in 1 M $LiClO_4$ in PC at various scanning rates. XPS spectra of $EV(PF_6)_2$ in (b) C 1s and (c) N 1s regions.

Owing to the large molecular weight and low density of organic active materials, it is difficult to achieve high-loading, or even under high-loading, the electrochemical performance will not be good. When preparing electrodes in this paper, EV-KB composite has been uniformly coated with carbon, so no additional conductive carbon is needed in the electrode slurry (Fig. S4a†); only polytetrafluoroethylene (PTFE) is needed to be mixed with EV-KB composite in the solvent for coating electrodes directly. The aluminum foil is commonly used in lithium batteries as the current collector. However, when it is adopted in the process of preparing EV-KB composite electrodes, it is difficult for slurry to be bonded with aluminum foil, which leads to its obvious separation from aluminum foil. Therefore, carbon paper is used as the current collector in this work to uniformly achieve a high-loading of 1.5–9 mg cm^{-2}. Due to its similar surface properties to active materials, carbon paper is more suitable for connection with EV-KB composite. In addition, the solvents in the slurry also have a great impact on the coating of electrodes. As shown in Fig. S5,† when *N*-methyl-2-pyrrolidone (NMP) is used, the coated electrodes will become severely cracked after drying, failing to achieve high-loading; however, when ethanol is used as the solvent, the electrodes will be uniformly distributed after drying, and there will be no cracks, achieving high-loading easily. This results demonstrated that it is also possible to optimize the current collectors and slurry solvents for the preparation of uniform organic active material based electrodes. Lithium metal is used as the reference electrodes and counter electrodes in this research to test the electrochemical performance of the EV-KB composite electrodes in CR2032 coin battery (Fig. S4b†).

The EV-KB composite electrode presents good rate capability and shows typical two-electron discharge–charge plateaus at various current densities (Fig. 4a). Meanwhile, as shown in Fig. 4b, under the current density range of 0.1–0.6 mA cm^{-2}, the EV-KB composite electrode realizes a specific capacity ranging from 101 to 65 mA h g^{-1}. Furthermore, after discharge–charge at high-rate current, the electrode can remain sound stability

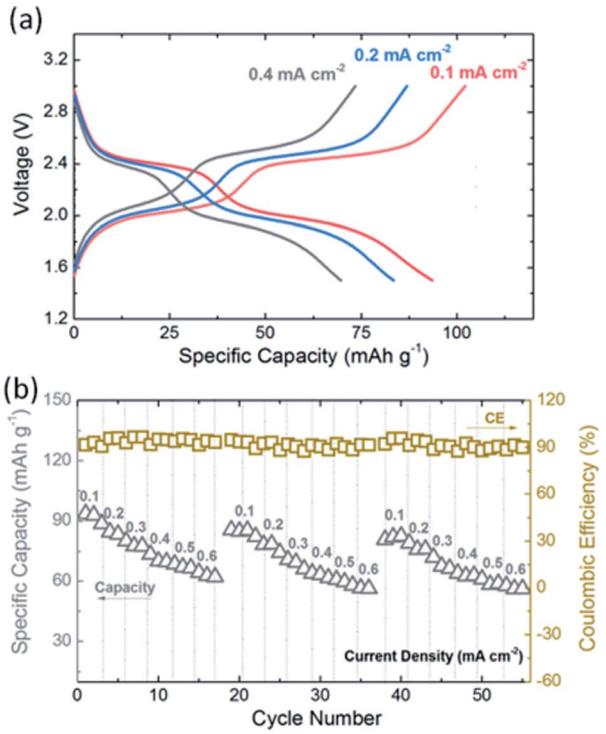

Fig. 4 (a) First galvanostatic discharge–charge profiles of EV-KB composite electrode between 0.1 and 0.4 mA cm^{-2}. (b) Rate capability and coulombic efficiency of the EV-KB composite electrode at various current densities from 0.1 to 0.6 mA cm^{-2}.

when returning to low-rate current with Coulomb efficiency higher than 95%, presenting good rate adaptability. By limiting the discharge–charge voltage, we also study the reversibility of the two-electron of the EV-KB composite electrodes respectively. By setting the discharge–charge voltage at the range of 2.1–3.0 V *vs.* Li/Li^+, it can be seen that the first electron (EV/EV^+) achieves 600 stable cycles with Coulomb efficiency about 98% (Fig. S6†). Likewise, when the range of discharge–charge voltage is set as 1.5–2.4 V *vs.* Li/Li^+, the second electron (EV/EV^+) can also realize 600 stable cycles with Coulomb efficiency of 98% (Fig. S7†). The two-electron discharge–charge plateau of viologen active materials brings better adaptability, which enables the materials to match with anode and cathode materials with various potentials.

Organic active materials generally have large molecular weight and small density, making it difficult to demonstrate good electrode performance at high-loading. Therefore, a relative large gap exists between the organic active materials and the commonly-used inorganic electrode materials for lithium batteries. However, high-loading is practically significant to the industrial application of organic electrodes. In this work, by optimizing the electrode current collector and slurry solvent, the EV-KB composite electrode successfully achieves stable performance at high-loading. Fig. 5a shows first galvanostatic discharge–charge profiles of EV-KB composite electrode at various loadings. When the electrode loading is between 1.5–9 mg cm^{-2}, the reachable specific capacity range is 106–79 mA h g^{-1}; *i.e.*, when the loading is increased by 6 times, the specific capacity can reach up to 75% of the theoretical value, which represents a relatively high level among the demonstrated organic electrodes at high-loading by far. Meanwhile, we realize 400 stable cycles at loading of 3 mg cm^{-2} with Coulomb efficiency of 96% (Fig. 5b), with the capacity decayed only 0.049% on each cycle. Moreover, stable cycle performance and rate capability are achieved at other high-loading as well (Fig. S8 & S9†). We also used the EV-KB composite electrode in a self-made pouch cell to further examine its applicability in the larger system. The galvanostatic discharge–charge profiles of EV-KB composite electrode with area of 4 × 2 cm^2 were shown in Fig. S10,† which still indicates the reasonable cycling stability and high coulombic efficiency. We believe that the performance of a larger battery system can be further improved by better cell design and manufacturing process.

As illustrated in Table 1, compared with recently-reported organic electrode materials,[32,53–65] the EV-KB composite organic electrode demonstrated in this paper reaches relatively high-loading (1.5–9 mg cm^{-2}), which represents a currently leading level. Meanwhile, it shows the reasonable cycle life among all organic electrodes. The demonstration of this stable and high-loading electrode is practically significant to the industrial application of organic active materials. The salification method adopted in this paper, which can effectively reduce the solubility of soluble viologen active materials in electrolyte

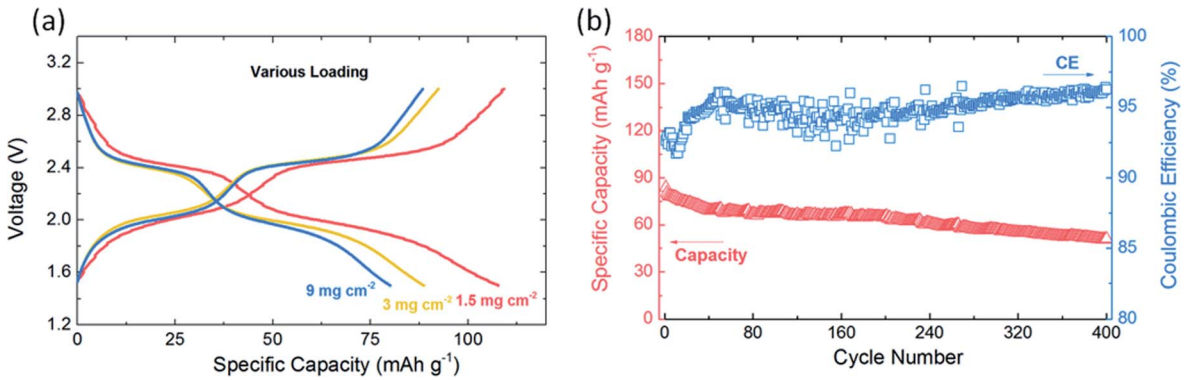

Fig. 5 (a) First galvanostatic discharge–charge profiles of EV-KB composite electrode at various mass loading at 0.2 mA cm^{-2}. (b) Capacity retention and coulombic efficiency of EV-KB composite electrode of mass loading ~3 mg cm^{-2} at 0.2 mA cm^{-2}.

Table 1 Performance parameters comparison of various organic electrodes

Active materials	Voltage (*vs.* Li/Li$^+$)	Specific capacity (mA h g^{-1})	Cycle life (No.)	Loading (mg cm^{-2})	Ref.
EV(PF$_6$)$_2$	2.4 & 2.0 V	106	400	1.5–9	This work
PTCLi$_4$	1.1 V	110	200	12	53
DMTS	2.2 V	720	50	6.7	54
PAQS	2.2 V	165	100	1–2	55
PDBS	2.5 V	200	20	1–2	56
Li$_2$PDHBQS	2.0 V	247	>1000	1–2	56
PBQS	2.7 V	275	>1000	1–2	57
2HNAQ	2.4 V	280	1000	2–3	58
PID	2.7 V	207	100	1.6	59
P14AQ	2.1 V	263	100	1–2	60
LiDHAQS	2.5 V	330	400	1	61
PBDTD	2.5 V	200	250	2–3	62
DAAQ-TFP	2.4 V	107	>1000	0.45	63
Li$_2$C$_8$H$_4$O$_4$	0.8 V	300	50	8–10	32
Li$_2$TDC	0.65 V	200	50	5	64
2,6-Naph(COOLi)$_2$	0.8 V	220	100	2.5	65

thus to enable their application in lithium batteries, can also be applied in other kinds of organic active materials. Furthermore, the high-energy ball milling, a simple and effective composite synthesizing method, provides a direction to further optimize the organic electrode performance and loading.

Conclusions

In summary, by adopting 4,4′-bipyridine as the raw material and combining salification with high-energy ball milling, a low-solubility and high-stability viologen carbon-coated EV-KB composite is synthesized in this research. Then, by optimizing the electrode preparation process, a high-loading viologen-based organic active material electrode is successfully prepared. Salification can effectively reduce the solubility of organic active materials in the electrolytes, thus enable the application of viologen active materials in lithium batteries. The importance of current collectors and slurry solvents is discussed in this research. By selecting carbon paper as the current collector and ethanol as the solvent, the EV-KB composite electrode with a loading up to 1.5–9 mg cm^{-2} is successfully prepared. This high-loading electrode can stably cycle 400 times at coulombic efficiency of 96%, achieving a specific capacity of 106–79 mA h g^{-1}, and it exhibits a good rate capability. The synthesis method and electrode preparation optimization process introduced in this paper provide a reference for other types of organic active materials to be used in high-loading lithium batteries.

Conflicts of interest

There are no conflicts to declare.

Acknowledgements

The work described in this paper was substantially supported by grants from the National Natural Science Foundation of China (Project No. 21908147 and No. 52076142), Natural Science Foundation of SZU (Grant No. 000002110234), the Shenzhen Science and Technology Fund (RCBS20200714114919158 and JCYJ20170818093905960).

Notes and references

1 B. Dunn, H. Kamath and J. M. Tarascon, *Science*, 2011, **334**, 928–935.
2 K. J. Griffith, K. M. Wiaderek, G. Cibin, L. E. Marbella and C. P. Grey, *Nature*, 2018, **559**, 556–563.
3 B. Scrosati, J. Hassoun and Y. K. Sun, *Energy Environ. Sci.*, 2011, **4**, 3287–3295.
4 B. Scrosati and J. Garche, *J. Power Sources*, 2010, **195**, 2419–2430.
5 Y. Liang, Y. Jing, S. Gheytani, K.-Y. Lee, P. Liu, A. Facchetti and Y. Yao, *Nat. Mater.*, 2017, **16**, 841–848.
6 J.-M. Tarascon and M. Armand, *Nature*, 2011, **414**, 171–179.
7 S. Zhang, S. Ren, D. Han, M. Xiao, S. Wang, L. Sun and Y. Meng, *ACS Appl. Mater. Interfaces*, 2020, **12**, 36237–36246.
8 A. Manthiram, *J. Phys. Chem. Lett.*, 2011, **2**, 176–184.
9 X. Shen, H. Liu, X.-B. Cheng, C. Yan and J.-Q. Huang, *Energy Storage Materials*, 2018, **12**, 161–175.
10 D. Larcher and J.-M. Tarascon, *Nat. Chem.*, 2015, **7**, 19–29.
11 Y. Li, Y. Lu, C. Zhao, Y.-S. Hu, M.-M. Titirici, H. Li, X. Huang and L. Chen, *Energy Storage Materials*, 2017, **7**, 130–151.
12 H. Chen, G. Cong and Y. C. Lu, *J. Energy Chem.*, 2018, **27**, 1304–1325.
13 X. Wu, S. Jin, Z. Zhang, L. Jiang, L. Mu, Y.-S. Hu, H. Li, X. Chen, M. Armand and L. Chen, *Sci. Adv.*, 2015, **1**, e1500330–e1500339.
14 Z. Song and H. Zhou, *Energy Environ. Sci.*, 2013, **6**, 2280–2301.
15 S. Lee, G. Kwon, K. Ku, K. Yoon, S. K. Jung, H. D. Lim and K. Kang, *Adv. Mater.*, 2018, **30**, 1704682–1704727.
16 T. B. Schon, B. T. McAllister, P.-F. Li and D. S. Seferos, *Chem. Soc. Rev.*, 2016, **45**, 6345–6404.
17 A. Shimizu, K. Takenaka, N. Handa, T. Nokami, T. Itoh and J.-I. Yoshida, *Adv. Mater.*, 2017, **29**, 1606592–1606597.

18 B. Huskinson, M. P. Marshak, C. Suh, S. Er, M. R. Gerhardt, C. J. Galvin, X. Chen, A. Aspuru-Guzik, R. G. Gordon and M. J. Aziz, *Nature*, 2014, **505**, 195–198.
19 E. J. Son, J. H. Kim, K. Kim and C. B. Park, *J. Mater. Chem. A*, 2016, **4**, 11179–11202.
20 H. Chen, M. Armand, G. Demailly, F. Dolhem, P. Poizot and J. M. Tarascon, *ChemSusChem*, 2008, **1**, 348–355.
21 G. Milczarek and O. Inganäs, *Science*, 2012, **335**, 1468–1471.
22 J. Hong, M. Lee, B. Lee, D.-H. Seo, C. B. Park and K. Kang, *Nat. Commun.*, 2014, **5**, 1–9.
23 X. Wei, W. Xu, M. Vijayakumar, L. Cosimbescu, T. Liu, V. Sprenkle and W. Wang, *Adv. Mater.*, 2014, **26**, 7649–7653.
24 T. Liu, X. Wei, Z. Nie, V. Sprenkle and W. Wang, *Adv. Energy Mater.*, 2016, **6**, 1501449.
25 K. Takechi, Y. Kato and Y. Hase, *Adv. Mater.*, 2015, **27**, 2501–2506.
26 C. DeBruler, B. Hu, J. Moss, X. Liu, J. Luo, Y. Sun and T. L. Liu, *Chem*, 2017, **3**, 961–978.
27 B. Hu and T. L. Liu, *J. Energy Chem.*, 2018, **27**, 1326–1332.
28 L. Liu, Y. Yao, Z. Wang and Y.-C. Lu, *Nano Energy*, 2021, **84**, 105897.
29 K. Amin, Q. Meng, A. Ahmad, M. Cheng, M. Zhang, L. Mao, K. Lu and Z. Wei, *Adv. Mater.*, 2018, **30**, 1703868–1703876.
30 I. A. Rodríguez-Pérez and X. Ji, *ACS Energy Lett.*, 2017, **2**, 1762–1770.
31 G. Dai, Y. He, Z. Niu, P. He, C. Zhang, Y. Zhao, X. Zhang and H. Zhou, *Angew. Chem.*, 2019, **131**, 10007–10011.
32 M. Armand, S. Grugeon, H. Vezin, S. Laruelle, P. Ribière, P. Poizot and J.-M. Tarascon, *Nat. Mater.*, 2009, **8**, 120–125.
33 É. Deunf, P. Moreau, É. Quarez, D. Guyomard, F. Dolhem and P. Poizot, *J. Mater. Chem. A*, 2016, **4**, 6131–6139.
34 C. Luo, X. Ji, J. Chen, K. J. Gaskell, X. He, Y. Liang, J. Jiang and C. Wang, *Angew. Chem.*, 2018, **130**, 8703–8707.
35 T. Ma, L. Liu, J. Wang, Y. Lu and J. Chen, *Angew. Chem.*, 2020, **132**, 11630–11636.
36 F. Wu, M. Liu, Y. Li, X. Feng, K. Zhang, Y. Bai, X. Wang and C. Wu, *Electrochem. Energy Rev.*, 2021, 1–65.
37 Y. Lu, Q. Zhang, L. Li, Z. Niu and J. Chen, *Chem*, 2018, **4**, 2786–2813.
38 S. H. Chung, P. Han, C. H. Chang and A. Manthiram, *Adv. Energy Mater.*, 2017, **7**, 1700537.
39 H. Yang, Z. Feng, X. Teng, L. Guan, H. Hu and M. Wu, *InfoMat*, 2021, 1–17.
40 A. Molina, N. Patil, E. Ventosa, M. Liras, J. Palma and R. Marcilla, *ACS Energy Lett.*, 2020, **5**, 2945–2953.
41 Y. Hu, W. Chen, T. Lei, Y. Jiao, J. Huang, A. Hu, C. Gong, C. Yan, X. Wang and J. Xiong, *Adv. Energy Mater.*, 2020, **10**, 2000082.
42 Y. Lu and J. Chen, *Nat. Rev. Chem.*, 2020, **4**, 127–142.
43 J. Liu, J. G. Zhang, Z. G. Yang, J. P. Lemmon, C. Imhoff, G. L. Graff, L. Y. Li, J. Z. Hu, C. M. Wang, J. Xiao, G. Xia, V. V. Viswanathan, S. Baskaran, V. Sprenkle, X. L. Li, Y. Y. Shao and B. Schwenzer, *Adv. Funct. Mater.*, 2013, **23**, 929–946.
44 Y. Yang, G. Y. Zheng and Y. Cui, *Chem. Soc. Rev.*, 2013, **42**, 3018–3032.
45 Y. Zhao, Y. Ding, Y. Li, L. Peng, H. R. Byon, J. B. Goodenough and G. Yu, *Chem. Soc. Rev.*, 2015, **44**, 7968–7996.
46 R. Marom, S. F. Amalraj, N. Leifer, D. Jacob and D. Aurbach, *J. Mater. Chem.*, 2011, **21**, 9938–9954.
47 G. Y. Zheng, Y. Yang, J. J. Cha, S. S. Hong and Y. Cui, *Nano Lett.*, 2011, **11**, 4462–4467.
48 H. Chen, Y. Zhou and Y.-C. Lu, *ACS Energy Lett.*, 2018, **3**, 1991–1997.
49 X. Zhao, C.-H. Yim, N. Du and Y. Abu-Lebdeh, *Ind. Eng. Chem. Res.*, 2018, **57**, 9062–9074.
50 P. Parikh, M. Sina, A. Banerjee, X. Wang, M. S. D'Souza, J.-M. Doux, E. A. Wu, O. Y. Trieu, Y. Gong and Q. Zhou, *Chem. Mater.*, 2019, **31**, 2535–2544.
51 L. Zhang, C. Zhang, Y. Ding, K. Ramirez-Meyers and G. Yu, *Joule*, 2017, **1**, 623–633.
52 M. Lee, J. Hong, J. Lopez, Y. Sun, D. Feng, K. Lim, W. C. Chueh, M. F. Toney, Y. Cui and Z. Bao, *Nat. Energy*, 2017, **2**, 861–868.
53 A. Iordache, D. Bresser, S. Solan, M. Retegan, M. Bardet, J. Skrzypski, L. Picard, L. Dubois and T. Gutel, *Adv. Sustainable Syst.*, 2017, **1**, 1600032–1600042.
54 M. Wu, Y. Cui, A. Bhargav, Y. Losovyj, A. Siegel, M. Agarwal, Y. Ma and Y. Fu, *Angew. Chem.*, 2016, **128**, 10181–10185.
55 Z. Song, T. Xu, M. L. Gordin, Y.-B. Jiang, I.-T. Bae, Q. Xiao, H. Zhan, J. Liu and D. Wang, *Nano Lett.*, 2012, **12**, 2205–2211.
56 Z. Song, Y. Qian, X. Liu, T. Zhang, Y. Zhu, H. Yu, M. Otani and H. Zhou, *Energy Environ. Sci.*, 2014, **7**, 4077–4086.
57 Z. Song, Y. Qian, T. Zhang, M. Otani and H. Zhou, *Adv. Sci.*, 2015, **2**, 1500124–1500133.
58 J. Lee and M. J. Park, *Adv. Energy Mater.*, 2017, **7**, 1602279–1602287.
59 Y. Liang, P. Zhang, S. Yang, Z. Tao and J. Chen, *Adv. Energy Mater.*, 2013, **3**, 600–605.
60 Z. Song, Y. Qian, M. L. Gordin, D. Tang, T. Xu, M. Otani, H. Zhan, H. Zhou and D. Wang, *Angew. Chem.*, 2015, **127**, 14153–14157.
61 A. Petronico, K. L. Bassett, B. G. Nicolau, A. A. Gewirth and R. G. Nuzzo, *Adv. Energy Mater.*, 2018, **8**, 1700960–1700967.
62 Y. Jing, Y. Liang, S. Gheytani and Y. Yao, *Nano Energy*, 2017, **37**, 46–52.
63 S. Wang, Q. Wang, P. Shao, Y. Han, X. Gao, L. Ma, S. Yuan, X. Ma, J. Zhou and X. Feng, *J. Am. Chem. Soc.*, 2017, **139**, 4258–4261.
64 W. Walker, S. Grugeon, H. Vezin, S. Laruelle, M. Armand, F. Wudl and J.-M. Tarascon, *J. Mater. Chem.*, 2011, **21**, 1615–1620.
65 T. Yasuda and N. Ogihara, *Chem. Commun.*, 2014, **50**, 11565–11567.